Networks of Ultrasmall Pd/Cr Nanowires as High Performance Hydrogen Sensors

Xiao-Qiao Zeng,[†,‡] Yong-Lei Wang,[†,§] Henry Deng,[⊥] Michael L. Latimer,[†,§] Zhi-Li Xiao,[†,§,*] John Pearson,[†] Tao Xu,[†,‡] Hsien-Hau Wang,[†] Ulrich Welp,[†] George W. Crabtree,[†,∥] and Wai-Kwong Kwok[†]

[†]Materials Science Division, Argonne National Laboratory, Argonne, Illinois 60439, United States, [‡]Department of Chemistry and Biochemistry and [§]Department of Physics, Northern Illinois University, DeKalb, Illinois 60115, United States, [⊥]Illinois Mathematics and Science Academy, Aurora, Illinois 60506, United States, and [∥]Departments of Physics, Electrical and Mechanical Engineering, University of Illinois at Chicago, Illinois 60607, United States

ABSTRACT The newly developed hydrogen sensor, based on a network of ultrasmall pure palladium nanowires sputter-deposited on a filtration membrane, takes advantage of single palladium nanowires' characteristics of high speed and sensitivity while eliminating their nanofabrication obstacles. However, this new type of sensor, like the single palladium nanowires, cannot distinguish hydrogen concentrations above 3%, thus limiting the potential applications of the sensor. This study reports hydrogen sensors based on a network of ultrasmall Cr-buffered Pd (Pd/Cr) nanowires on a filtration membrane. These sensors not only are able to outperform their pure Pd counterparts in speed and durability but also allow hydrogen detection at concentrations up to 100%. The new networks consist of a thin layer of palladium deposited on top of a Cr adhesion layer 1−3 nm thick. Although the Cr layer is insensitive to hydrogen, it enables the formation of a network of continuous Pd/Cr nanowires with thicknesses of the Pd layer as thin as 2 nm. The improved performance of the Pd/Cr sensors can be attributed to the increased surface area to volume ratio and to the confinement-induced suppression of the phase transition from Pd/H solid solution (α-phase) to Pd hydride (β-phase).

KEYWORDS: hydrogen sensor · palladium · chromium · nanowire · network

Hydrogen (H_2) gas has many uses. For example, it is the main propellant in spaceships and commercial and military launch vehicles. It is also used extensively in scientific research and industry, notably in the manufacturing of glass and steel as well as in the refining of petroleum products.[1] In 2003, the U.S. Department of Energy accelerated its hydrogen program to develop the technology needed for commercially viable hydrogen-powered fuel cells—a way to power cars, trucks, homes, and businesses that could significantly reduce pollution and greenhouse gas emissions as well as our dependence on fossil fuels.[2] However, H_2 gas is highly volatile and, when in contact with oxygen, can become extremely flammable and highly explosive. The use of effective H_2 sensors to accurately and quickly respond to H_2 gas leaks and to monitor manufacturing and distribution will be crucial for the safe deployment of all H_2-based applications. For example, H_2 gas detection in commercial and military launch vehicles is a great concern at both the propellant-filling ground-support station and within the common booster core during ground operations.[3] Fuel cells[4] at the core of hydrogen-powered cars require two types of H_2 sensors: sensors to monitor the quality of the hydrogen feed gas and, more importantly, sensors to detect leaks. These H_2 sensors must be sensitive enough to discriminate between ambient low-level traces of hydrogen and those that are generated by a H_2 leak.[5] A crucial parameter of H_2 sensors in many applications is the response time. For example, the sensors that analyze H_2 content in a mixed gas and monitor the reaction process require extremely short response times to follow the fuel cell's power generation and to shut down the engine in the event of a tank rupture. Currently, commercial sensors suffer from longer response times than the duty cycles likely needed for most applications.[5,6]

Intensive research has been conducted in recent years to develop a new generation of H_2 sensors with high speed, high sensitivity, miniature size, and low cost.[6−36] Nanomaterials[7−31] have been a major focus in the search for high-performance H_2 sensing elements due to their large surface area to volume (SA/V) ratios which could enhance the absorption/desorption rates of a chemical reaction and allow for shorter H_2 diffusion paths as well as confinement-induced new properties. Among the various nanomaterials available, palladium (Pd) nanostructures[7,8,13,18,22−24,26,27] have shown very promising properties suitable for fast H_2 sensors. Pd-based H_2 sensors have a unique advantage in that the surface of palladium

* Address correspondence to xiao@anl.gov, zxiao@niu.edu.

Received for review June 27, 2011 and accepted August 21, 2011.

Published online August 22, 2011
10.1021/nn2023717

© 2011 American Chemical Society

can act catalytically to break the H−H bond in diatomic hydrogen, allowing monatomic hydrogen to diffuse into the material. Furthermore, palladium can dissolve more than 600 times its own volume of hydrogen but dissolves little of the other common gases such as nitrogen, oxygen, nitrogen monoxide, carbon dioxide, and carbon monoxide. This allows Pd to be the most selective H_2 sensing material.[6] Finally, the Pd hydrogenation process is reversible at room temperature, enabling simpler designs and allowing for less power consumption by avoiding heating to achieve elevated temperatures.

Continuous Pd nanowires which respond to H_2 with an increase in resistance have been achieved through various nanofabrication techniques and have been systematically investigated.[8,9,22−24,26,27] Both experimental and simulation results show that their H_2 sensing ability increases and their response time decreases when the sensors' transverse dimensions shrink. The results clearly demonstrate that Pd nanowires can be excellent sensing elements for highly sensitive and fast acting H_2 sensors. The utilization of single palladium nanowires, however, faces challenges in nanofabrication, manipulation, and achieving ultrasmall transverse dimensions. Recently, we developed a new fabrication method[37] that takes advantage of single palladium nanowires' high speed and sensitivity while eliminating the nanofabrication obstacles; high-performance H_2 gas sensors were achieved by sputter-depositing pure palladium onto commercially available and inexpensive filtration membranes. This nanomanufacturing approach could enable a potential scale-up of Pd-nanowire-based H_2 sensors for industrial applications.

Previous results have shown that the response of the Pd nanowire network sensors become faster when the thickness of the network is reduced.[37] However, a crossover from continuous to broken nanowire networks occurs at a certain critical thickness, similarly to what has been observed in ultrathin Pd films,[1,13] limiting the potential for further decreasing the response time through reduction of the network thickness. These newly developed Pd nanowire network sensors also inherit the drawback of the single Pd nanowire: an inability to distinguish H_2 concentrations above 3%. This deficiency of the sensor definitely hinders its potential applications, for example, in a fuel processor and as a safety monitor in a vehicle which require the device to be sensitive to hydrogen in the range 1−100 and 0.1−10%, respectively.[38] Here we report experiments aiming to further improve the performance of this type of H_2 sensor by reducing the thickness of the network while enabling the Pd nanowires to be continuous. By first depositing a layer of chromium (Cr) with a thickness of 1−3 nm onto the filtration membrane substrate, we create networks of Pd/Cr nanowires with the thickness of the continuous palladium layer as low as 2 nm. These Pd/Cr nanowire networks are faster than the pure palladium counterparts in responding to H_2 gas. The excellent adhesion of Cr to the substrate also helps to significantly improve the durability of the sensor. Even more importantly, the Pd/Cr sensors are able to distinguish H_2 concentrations up to 100%, eliminating a crucial drawback of its pure palladium counterparts. Since this change can be attributed to the confinement-induced suppression of a phase transition in the Pd/H system, our results demonstrate that the performance of H_2 sensors based on Pd nanostructures can indeed go beyond the benefits expected from the increased SA/V ratios and shorter diffusion distances.

RESULTS AND DISCUSSION

When a metal is deposited onto a nonmetallic substrate, it initially tends to nucleate into fine particles. The morphology of the particles is governed by the minimization of the surface free energy.[39,40] Using the equilibrium of surface tension, one can write $\gamma_{sg} = \gamma_{ms} + \gamma_{mg} \cos\theta$, where θ is the contact angle between the particle and the substrate, γ is the surface or interfacial energy, and the subscripts s, m, and g stand for substrate, metal particle, and gas, respectively. If the metal−substrate interfacial energy γ_{ms} is smaller than the surface energy of the substrate γ_{sg}, θ will be smaller than 90°. In this case, the supported particle will tend to have a half-dome shape or even spread over to have a raft-like morphology. If γ_{sg} is smaller than γ_{ms}, then θ will be greater than 90°, and the particles tend to appear spherical or polyhedral. In the latter case, the layer of metal must reach a θ dependent critical thickness to form a continuous film on the substrate. A crossover from continuous to discontinuous behavior was observed in Pd films on Si_3N_4 and SiO_2 substrates at thicknesses of 4 and 5 nm, respectively.[1,13]

Porous Anodisc filtration membranes from Whatman—the substrates used to form Pd nanowire networks—are made of anodic aluminum oxide.[37,41] It is well-known that the Pd/Al_2O_3 system has weak metal−substrate interaction.[39,40] Thus, a Pd layer on an alumina substrate may be continuous only when it achieves critical thickness. Indeed, the H_2 response of this newly developed pure Pd nanowire network sensor depends strongly on the thickness of the Pd layer:[37] at 7 nm and thicker, the network consisting of continuous Pd nanowires has a shorter response time when its thickness is reduced. At 4 nm and below, the majority of the Pd nanowires become discontinuous and the H_2-induced resistance changes of the network are dominated by broken Pd nanowires, leading to a retarded H_2 response. We also found coexistence of continuous and broken Pd nanowires at thicknesses of 4 nm < d < 7 nm, where resistance changes contributed from broken and continuous Pd nanowires compete, which is consistent with

observations on ultrathin Pd films on polymer (SU8) substrates.[29]

Crispin *et al.* found that the contact angle between Ni and alumina can be significantly reduced by adding a small amount of chromium. For example, the contact angle is close to 90° on both sapphire and polycrystalline alumina with 10% Cr in Ni and is ~75° with 20% Cr.[42,43] Here we demonstrate that an addition of a Cr buffer layer as thin as 1 nm between Pd and alumina substrates (Anodisc filtration membranes) can modify the Pd−substrate interaction and reduce the critical thickness of the Pd layer required to form a continuous Pd layer. We were able to achieve networks of continuous Pd nanowires with thicknesses down to 2 nm on Anodisc filtration membranes.

Figure 1 presents a typical top-view scanning electron microscopy (SEM) micrograph of a Pd/Cr nanowire network (sample S1) deposited onto an Anodisc13 membrane with an effective filtration pore diameter of 20 nm. The image was taken of a Pd/Cr sample with a nominal thickness of 2 nm for both the deposited Pd and Cr. As listed in Table 1, we conducted experiments on Pd/Cr nanowire network samples (samples S1−S9) with thickness ranging from 1 to 3 nm for the Cr layer and from 2 to 7 nm for the Pd layer with a thickness step of 1 nm. Since the deposited Pd/Cr layer is thin (<10 nm), the morphology of the network simply duplicates that of the bare filtration membrane.[37,41] The widths of the Pd/Cr nanowires (*i.e.*, sections between the pores) in Figure 1 are 7−9 nm. A cross-section SEM imaging finds no metal inside the pores, consistent with those reported in networks of pure Pd nanowires on filtration membranes[37] and in other perforated films sputter-deposited on nanoporous alumina substrates.[44,45]

The resistance of a network of pure Pd nanowires was found to decrease (or decrease after an initial positive surge) in the presence of H_2 when its thickness was reduced to less than 7 nm.[37] That is, its H_2 responses are dominated (or affected) by broken Pd nanowires which can become continuous and more conductive due to hydrogen-induced dilation of Pd grains.[13,37] However, in our Pd/Cr nanowire networks, which consist of a Pd layer thinner than 7 nm, the resistance increases when exposed to various concentrations of H_2, as indicated by the data presented in Figure 2 for samples S2 and S3 based on a 2 nm Pd/3 nm Cr network. It is evident that the resistance of the sample initially increases with time and then saturates at a value that depends on the H_2 concentration. Experimentally, we did not observe hydrogen-induced resistance changes in the control samples (samples C1−C4), with only Cr deposited on both filtration membranes and Si substrates. Furthermore, a gap closing between neighboring Pd clusters or Pd and Cr clusters due to the dilation of Pd clusters in the presence of hydrogen will decrease the resistance of the nanowires. Thus, the observed resistance increase of the Pd/Cr nanowire networks should originate from the formation of Pd/H solid solution (at low H_2 concentrations) or Pd hydride (at high concentrations).[9,26,27,37] This also implies that the Pd nanowire networks are continuous.

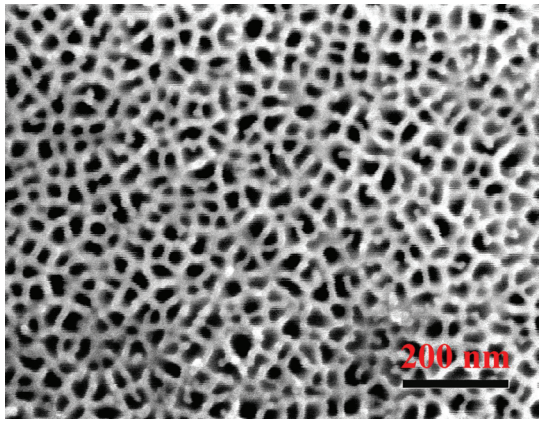

Figure 1. Scanning electron microscopy (SEM) image of a 2 nm Pd/2 nm Cr nanowire network (sample S1) coated on an Anodisc13 alumina membrane with a nominal filtration pore diameter of 20 nm. The thicknesses of the deposited Pd and Cr layers are 2 nm each. The scale bar is 200 nm.

TABLE 1. Baseline Resistances (R_0) of the Pd/Cr Nanowire Network Sensors

samples	S1	S2	S3	S4	S5	S6	S7	S8	S9
d_{Cr}[a] (nm)	2	3	3	2	1	2	2	2	2
d_{Pd}[a] (nm)	2	2	2	4	2	3	4	6	7
R_0 (kΩ)	5.941	3.038	2.235	1.290	7.806	3.800	1.284	0.826	0.381

[a] Values of d_{Cr} and d_{Pd} are the nominal thicknesses of the deposited Cr and Pd layers, respectively.

The dramatic effect of the Cr buffer layer on the performance of the Pd-based network sensors can be clearly seen in Figure 3, which presents a comparison of the H_2 responses for a 4 nm thick Pd nanowire network (sample C5) with a 2 nm Pd/2 nm Cr network (sample S1). Although the total thicknesses of these two networks are identical, their baseline resistances in the absence of H_2 differ by a factor of more that 3 orders of magnitudes: the resistance of the 4 nm Pd sample is as high as 10 MΩ, while the replacement of 2 nm thick Pd with a 2 nm thick Cr layer reduces the resistance to a few kΩ, as shown by the data presented in Figure 3a,b and Tables 1 and 2. Since Cr has higher electrical resistivity than Pd,[46,47] such an enormous reduction of the sample resistance by the Cr layer implies a change in the morphology of the Pd/Cr nanowires from that of the pure Pd ones. That is, the 4 nm thick pure Pd network probably consists of broken nanowires, while the 2 nm Pd/2 nm Cr networks should be continuous. Such a change in morphology is reflected in the H_2 responses: the resistance

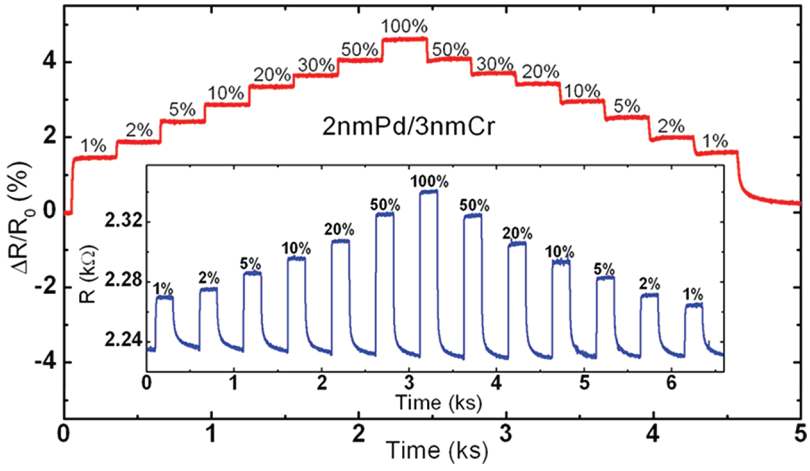

Figure 2. Responses of 2 nm Pd/3 nm Cr nanowire networks to hydrogen gas of various concentrations. ΔR is defined as the absolute resistance change $R(t) - R_0$, where R_0 is the baseline resistance in the absence of hydrogen gas. The data presented in the main panel and in the inset are from samples S2 and S3, respectively.

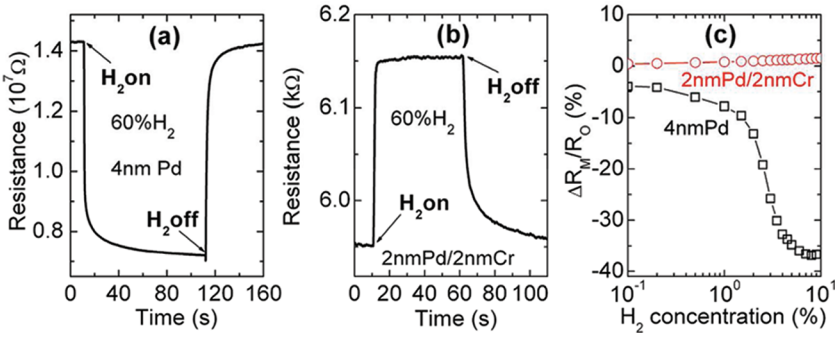

Figure 3. Comparisons of the hydrogen responses of a bare 4 nm Pd (sample C5) and a 2 nm Pd/2 nm Cr (sample S1) nanowire network which have the same total thicknesses: (a,b) evolution of the resistance with time at a fixed concentration of 60% and (c) maximal resistance change $\Delta R_M/R_0$ at various concentrations. R_0 is the baseline resistance in the absence of hydrogen gas, and ΔR_M is defined as the maximal resistance change $\Delta R = R(t) - R_0$ at the steady state for a specific concentration.

of the 2 nm Pd/2 nm Cr sample (sample S1) increases when exposed to H_2, in contrast to that of the 4 nm thick pure Pd sample (sample C5) for the same H_2 concentration, as indicated by the data presented in Figure 3a,b. The same behavior was observed for all tested H_2 concentrations, as demonstrated by the concentration dependences of the maximal resistance change $\Delta R_M/R_0$ given in Figure 3c for these two samples.

The above results clearly indicate that the Pd layer with a nominal thickness of only 2 nm is electrically connected in the Pd/Cr nanowires. This could be understandable if the Cr adhesion layer were continuous, resulting in a continuous Pd layer on top of it due to the complete wettability between two metals. Although a layer-by-layer growth of Cr films on alumina substrates with perfect surfaces was observed, a reduced surface promotes a three-dimensional (3D) growth process.[48] These results were attributed to the strong chemical interaction between Cr and the alumina surface and to the 3D nucleation on defect sites.[48] The extremely high resistances of our control samples with a Cr thickness of 2 nm or less on filtration membranes (samples C1 and C2 in Table 2) indicate that broken Cr nanowires dominate their electrical properties. This implies that the Cr layer on the alumina filtration membrane probably grows *via* a 3D nucleation process and may not be continuous when its thickness is 2 nm or less. Due to the strong chemical interaction between Cr and the alumina surface,[48] however, the Cr clusters should spread over a lager area than the Pd clusters for the same nominal layer thickness. Since the Pd on top of Cr will be continuous and it will be easier to fill the small gaps between neighboring Cr clusters with Pd, this can lead to a

TABLE 2. Baseline Resistances (R_0) of the Comparison Samples

samples	C1	C2	C3	C4	C5	C6	C7
substrates	filter	filter	filter	Si	filter	filter	Si
d_{Cr}[a] (nm)	1	2	3	1	0	0	2
d_{Pd}[a] (nm)	0	0	0	0	4	7	2
R_0 (kΩ)	8500	2600	28.10	2.401	14290	2.089	0.123

[a] Values of d_{Cr} and d_{Pd} are the nominal thicknesses of the deposited Cr and Pd layers, respectively.

decrease of the total thickness required to form continuous Pd nanowires. That is, a Cr layer of 2 nm or less in the Pd/Cr nanowires on the filtration membrane promotes the formation of a continuous Pd layer with a thickness less than that required in pure Pd nanowires, even though the Cr layer itself may be discontinuous. Furthermore, the Pd and Cr (or parts of them) may also form an alloy, similar to that observed in the Ni/Cr alloy,[42,43] which can have improved wettability on the filtration membrane than pure Pd, leading to a reduction in the critical thickness requirement for forming continuous Pd/Cr nanowires. It is clear that more research is needed to reveal the mechanism responsible for the reduction of the critical thickness induced by the Cr adhesion layer for forming continuous Pd and Pd/Cr layers.

When bulk Pd is exposed to hydrogen,[49] it forms a Pd/H solid solution (α-phase) and a Pd hydride (β-phase) at hydrogen contents (atomic ratios of H:Pd) less than α_M and higher than β_m, respectively. At room temperature, the values of α_M and β_m are 0.015 and 0.61, respectively. A mixed phase ($\alpha+\beta$ phase) exists at intermediate hydrogen content. The hydrogen-induced resistance change, which is the core of a Pd-based resistive H_2 sensor, is very sensitive to the hydrogen content in the α-phase and shows only a small increase from α_M up to β_m composition. In the β-phase region, the resistance first increases abruptly, reaching a value of 87% larger at $\sim\beta = 0.76$, and then stays nearly constant at higher hydrogen contents. The H_2 concentration dependence of the resistance change in thick Pd films follows a similar trend with the appearance of the pure β-phase at concentrations of 1−1.5%, depending on the thickness of the film.[36] Since the resistance of Pd in the majority portion of the pure β-phase does not change with H_2 concentration, a pure Pd-based sensor loses its sensitivity and, thus, is inapplicable at high H_2 concentrations (>2%).

Such saturation behavior was also reported for electrodeposited single Pd nanowires[26,27] and for networks of pure Pd nanowires formed on filtration membranes[37] where the sample resistance first increases with H_2 concentration up to about 1−2% and then remains constant at higher concentrations. The data shown in Figure 2 for the 2 nm Pd/3 nm Cr nanowire network, however, clearly show a difference in the resistance change induced by hydrogen with concentrations up to 100%. This observation is further summarized in Figure 4a where we plot the resistance change obtained at various H_2 concentrations. Quantitative analysis demonstrates that the concentration dependence of the maximal resistance change $\Delta R_M/R_0$ follows a power-law relation with an exponent of 0.26 for concentrations up to 100%. This indicates that the interaction of H_2 and Pd in the whole concentration range follows Sievert's law.[50] That is, the ratio of the dissolved atomic H_2 to Pd atoms can be described to a good approximation with a power-law dependence of

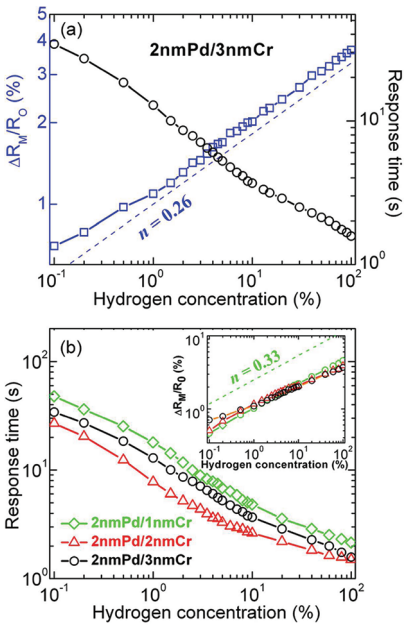

Figure 4. Concentration dependences of the response times and the maximal resistance changes $\Delta R_M/R_0$ for a 2 nm Pd/3 nm Cr nanowire network (sample S3) (a) and 2 nm Pd/1 nm Cr (sample S5), 2 nm Pd/2 nm Cr (sample S1), and 2 nm Pd/3 nm Cr (sample S3) (panel b and its inset). The response time is defined as the rise time to reach 90% of its maximal change, *i.e.*, $\Delta R/\Delta R_M = 0.9$. The dashed lines in (a) and in the inset of (b) represent a power-law relation with exponents of $n = 0.26$ and 0.33, respectively.

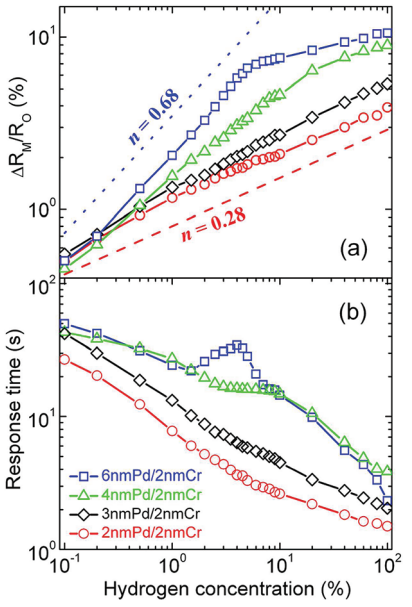

Figure 5. Concentration dependences of the maximal resistance change $\Delta R_M/R_0$ (a) and the response times (b) for 2 nm Pd/2 nm Cr (sample S1), 3 nm Pd/2 nm Cr (sample S6), 4 nm Pd/2 nm Cr (sample S7), and 6 nm Pd/2 nm Cr (sample S8) nanowire networks. The dashed and dotted lines in (a) represent a power-law relation with exponents of n = 0.28 and 0.68, respectively.

the H_2 partial pressure (*i.e.*, H_2 gas concentrations in our experiments), and the change of this ratio leads to a proportional $\Delta R_M/R_0$ response.[50] The exponent of n = 0.26 is smaller than the theoretical value of 0.5 and that (0.58) for a 7 nm thick pure Pd nanowire network.[37] This difference can be partially attributed to the H_2 insensitive resistance of the shunted Cr layer. This hypothesis is consistent with the observed exponent increase when the resistance contributed by the Cr layer is smaller, as demonstrated by the data obtained by either reducing the thickness of the Cr layer from 3 to 1 nm while keeping the thickness of the Pd layer at 2 nm (inset of Figure 4b) or increasing that of the Pd (Figure 5a) from 2 to 6 nm as the Cr layer stays at 2 nm thick. However, the change of n (from 0.28 to 0.68) induced by increasing the thickness of the Pd layer is much larger than that (from 0.26 to 0.33) by decreasing the thickness of the Cr layer, though the changes in the ratios of the thicknesses of Pd and Cr layers are the same. This indicates that the exponent n is strongly associated with the confinement effect due to the thickness reduction in the Pd layer.

The power-law dependence of the resistance change on the H_2 concentration implies that the 2 nm thick Pd nanowire network is in the α-phase for the whole concentration range and that the addition of a Cr buffer layer suppresses the α- to β-phase transition. The absence of the β-phase can also be inferred from the concentration dependence of the response time, which is defined as the rise time to reach 90% of its maximal change, as presented in Figure 4b for a series of Pd/Cr nanowire networks with various Cr layer thicknesses of 1, 2, and 3 nm. A peak or bump in the response time *versus* concentration relation was found to accompany the α- to β-phase transition in single Pd nanowires[26,27] and pure Pd nanowire networks.[37] However, the data in Figure 4b show a monotonic decrease of the response time with H_2 concentration up to 100%.

The survival of the α-phase at high H_2 concentrations can be a consequence of confinement effect. In fact, X-ray diffraction measurements on Pd nanoclusters reveal no α- to β-phase transition in 3.8 nm sized clusters.[51] Hydrogen solubility studies[52] on palladium clusters with diameters of 2−5 nm also show that nanoclusters in the α-phase can absorb 5−10 times more H_2 than bulk palladium, shifting the maximum hydrogen content (α_M) to a higher value. Hence, the concentration range of the α-phase is extended when the cluster size of Pd is reduced. Such an enhancement of the hydrogen solubility in the α-phase of Pd nanoclusters is attributed to the existence of subsurface sites for hydrogen atoms, in addition to the usual octahedral sites of the face centered cubic (fcc) Pd host lattice.[52] Although Pd forms a continuous nanowire network rather than separate nanoclusters in the

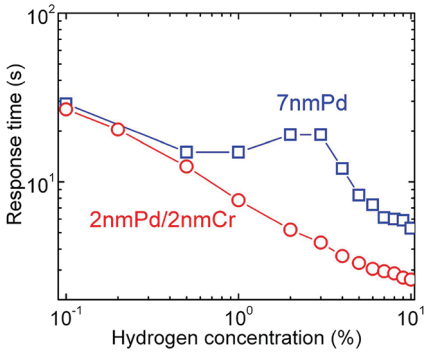

Figure 6. Comparison of the response times of a 2 nm Pd/2 nm Cr network (sample S1) with a bare 7 nm Pd nanowire network (sample C6) at various concentrations.

2 nm Pd/3 nm Cr sample, the confinement effect seems to be strong enough to sustain the α-phase up to H_2 concentrations of 100%. Since the width (7−9 nm) of the nanowires in the network is larger than the diameter (6 nm) of the nanoclusters in which α- to β-phase transition was observed,[47] the extension of the concentration range for the α-phase is due to the confinement in the thickness direction. In this case, the β-phase is expected to appear when the thickness of the nanowire network is increased. Figure 5 presents H_2 responses of Pd/Cr nanowire networks with various Pd layer thicknesses while maintaining a constant Cr buffer layer thickness. For samples with Pd thicknesses of 2 and 3 nm, the H_2 concentration dependence of the resistance change $\Delta R_M/R_0$ follows a power-law relation, and the response times also decrease monotonically with concentrations up to 100%. Thus, the α- to β-phase transition should be absent in the Pd/Cr nanowire networks with Pd layer thickness of 3 nm or less. When the thickness of the Pd layer is increased to 4 nm, the power-law dependence of the resistance change $\Delta R_M/R_0$ on concentration is valid up to a H_2 concentration of 8%. A bump also appears in the response time *versus* concentration curve. With further increase of the Pd thickness up to 6 nm, the deviation from the power-law relation in the $\Delta R_M/R_0$ *versus* concentration curve becomes more significant at H_2 concentration above 5%. A clear peak also emerges in the concentration dependence of the response time. These features are characteristics of the α- to β-phase transition and reveal the existence of the β-phase in the samples with 4 and 6 nm thick Pd layers. The observation of the α- to β-phase transition in these samples indicates that the Pd layer in the Pd/Cr networks behaves similarly to the nanoclusters,[51] electrodeposited single nanowires,[25,26] and nanowire networks[37] of pure Pd. This implies that pure Pd with at least one dimension (*e.g.*, thickness) of less than 4 nm could be sensitive to H_2 at concentrations up to 100%. Since the lattice expansion in the α-phase is extremely small, it will be extremely challenging to utilize the "gap closing" mechanism[8,13] to detect H_2. As observed in both films[1,29] and nanowire

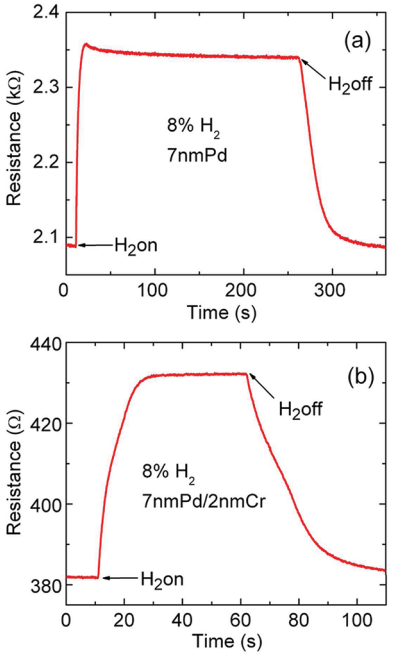

Figure 7. Comparison of the responses of a bare 7 nm Pd (sample C6) (a) and a 7 nm Pd/2 nm Cr (sample S9) (b) nanowire networks to 8% H_2.

networks[37] formed on bare substrates, however, a layer of pure Pd will become discontinuous when its thickness is reduced to less than 4 nm. Our success in fabricating a continuous Pd layer as thin as 2 nm by adding a thin buffer layer of Cr provides a new way to achieve Pd-based sensors, which can be sensitive to H_2 at concentrations of up to 100%.

It has been demonstrated in both single Pd nanowires[26] and Pd nanowire networks[37] that the surface area to volume (SA/V) ratio limits the response time of the sensor rather than the proton diffusion. This is because the proton diffusion time in a nanostructure is far shorter than any reported sensor response time. For example, Einstein's expression[26] yields a time of ~100 μs for a proton to diffuse a distance of 10 nm. Figure 6 presents a comparison of the fastest response times observed in a 2 nm Pd/2 nm Cr network and in a pure 7 nm thick Pd network. Though the 2 nm thick Pd network is indeed faster at all tested concentrations, the difference in the response times is definitely much shorter than that (by a factor of ~12) expected from a diffusion-limited process. Furthermore, the long response times in the 7 nm thick nanowire network at H_2 concentrations above 1% reflect a significant contribution from the α- to β-phase transition which causes a retarded H_2 response.[25,26] The difference (a factor of 1.08−1.21) in response times for these two samples in the α-phase (at H_2 concentrations less than 1%) is also smaller than that expected due to SA/V ratio increase (a factor of 1.82−1.98 by assuming a rectangular cross section for the Pd nanowires with a width of 7−9 nm). This disparity is probably caused by the

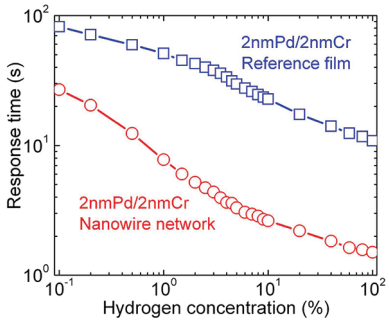

Figure 8. Comparison of the response times of a 2 nm Pd/2 nm Cr network (sample S1) with its reference film (sample C7) at various concentrations.

reduction of granularity in the 2 nm thick Pd nanowire network with a Cr buffer layer. The 7 nm thick Pd sample deposited on a bare oxide substrate should be more granular, and the grain boundaries serve as additional surfaces to interact with hydrogen. This hypothesis is in fact supported by the data presented in Figure 7: at a hydrogen concentration of 8%, the resistance of a 7 nm thick Pd nanowire network with a 2 nm thick buffer layer of Cr remains constant between 30 and 60 s, while that for the sample on bare substrate cannot reach a steady state after more than 250 s. The decrease of the resistance with time at a constant hydrogen concentration indicates that the 7 nm thick Pd nanowire network without a 2 nm thick buffer layer of Cr is granular and the hydrogen-induced Pd grain dilation enables more conducting paths when more gaps between neighboring grains are shortened with time.

The importance of surface area on the sensor response time is further demonstrated in Figure 8 where we compare the response times of a 2 nm Pd/2 nm Cr nanowire network and its reference film deposited simultaneously onto a silicon substrate (with a 300 nm thick oxide top layer). Since the shortest hydrogen diffusion distance of 2 nm (the thickness) is the same for both samples, the significant decrease of the response times in the network sample must come from the additional surface area of the porous substrate morphology. As discussed above, the growth mode of a Cr film can strongly depend on the roughness of the substrate surface.[48] In fact, this can be the origin of the pronounced difference in resistances of the 1 nm thick Cr samples deposited on a filtration membrane and a Si substrate (samples C1 and C4 in Table 2, respectively). That is, the morphology of the Pd layers on Cr-coated filtration membrane and Si substrate may not exactly be identical, resulting in different H_2 absorption kinetics. This could account for the dependence of the response times on H_2 concentration ratios in these two types of samples, as demonstrated by the data given in Figure 8.

Ostwald ripening, in which the larger clusters take up mobile atoms at the expense of smaller ones in a

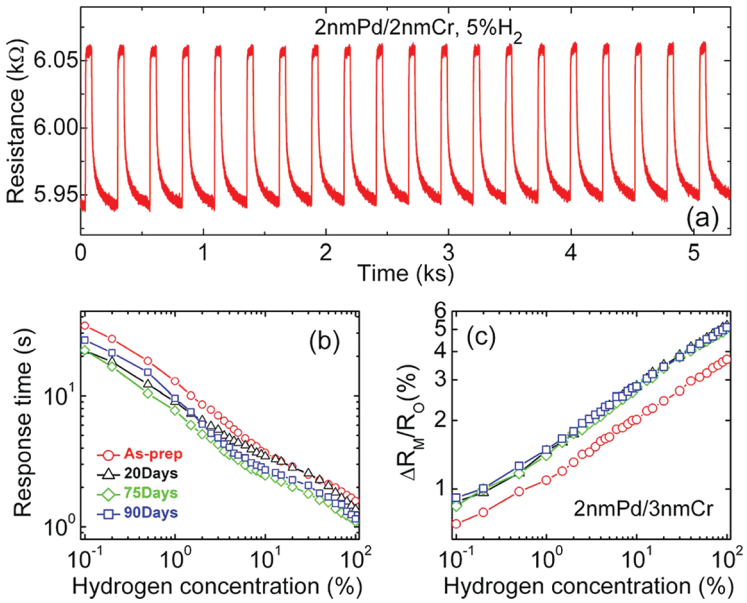

Figure 9. Data on the reversibility and durability. (a) Responses of a 2 nm Pd/2 nm Cr nanowire network (sample S1) to 5% hydrogen for 20 cycles. (b) Hydrogen concentration dependences of the response times and the maximal resistance changes $\Delta R_M/R_0$ of a 2 nm Pd/3 nm Cr nanowire network (sample S3) obtained shortly (within hours) after fabrication and stored in air for 20, 75, and 90 days.

nanocluster ensemble, is an extremely slow process at room temperature. However, the presence of a hydrogen atom in the metal lattice reduces the binding energy, thus increasing the probability of detachment of palladium atoms.[53] Recently Di Vece *et al.* reported hydrogen-induced Ostwald ripening at room temperature in a Pd nanocluster film.[53] Such a ripening process could also occur in our sputter-deposited Pd nanowire networks consisting of grains of various sizes, leading to irreversible hydrogen responses due to a morphological or structural change during a hydrogenation of the network. Figure 9a shows a resistance *versus* time curve for a 2 nm Pd/2 nm Cr nanowire network (sample S1) with 20 loading/unloading cycles. It is evident that the process is reversible: the resistance of the sample in the presence of hydrogen stays precisely the same for all cycles while it increases slightly when the hydrogen is replaced with nitrogen, probably due to the slow recovery which may require an even longer waiting time. This result, along with data presented in the inset of Figure 2 showing repeatable resistance change during hydrogen concentration sweeping, demonstrates that our Pd/Cr nanowire networks can respond to hydrogen reversibly, excluding the occurrence of Ostwald ripening. We also did not observe fracturing of the Pd/Cr nanowires after repeated exposures to H_2, in contrast to that reported for pure Pd nanowires.[22] This robustness of the Pd/Cr sensor may be a benefit of the strong chemical interaction between Cr and the alumina surface.[48]

In many applications, a hydrogen sensor needs to be exposed to air or an oxygen environment. Though the Cr layer is covered by the Pd layer on the top surface, it may oxidize by reacting with oxygen diffused in from the sides. Such a process in the Cr layer might have an impact on the morphology of the Pd layer and hence on the performance of the Pd/Cr hydrogen sensor. We addressed this issue by examining the hydrogen responses of a 2 nm Pd/3 nm Cr sensor (sample S3) just after preparation (and stored in a drybox for a few hours to make electrical contacts) and exposed to air for various periods of time. The results are presented in Figure 9b,c. Surprisingly, after storage in air, the sensor has a larger resistance change and a shorter response time compared to those of the pristine sample. That is, the performance of the sensor is improved by exposure to air. This indicates that due to the oxidation of the Cr layer the Pd layer may have more defects which can act as additional hydrogen interaction "surfaces". The oxidation process, however, should end after a period of time. Thus the sensor should become stable eventually, as demonstrated by the nearly identical resistance changes of the sensor stored in air after 20, 75, and 90 days (see Figure 9c). The slight difference in the concentration dependence of the response times obtained after 20 days or longer air exposure indicates subtle changes in the sensor.

CONCLUSIONS

In summary, we designed and achieved a new type of H_2 sensor based on networks of ultrasmall (<10 nm) palladium and chromium (Pd/Cr) nanowires sputter-deposited seqentially on commercially available and inexpensive alumina filtration membranes. While preserving the short response times of the previously reported pure palladium nanowire networks, the Pd/Cr

sensor can eliminate a crucial drawback of its predecessors, that is, their ability to distinguish H_2 concentrations only up to 3%. When the thickness of its Pd layer is 4 nm and below, the new sensor is capable of distinguishing hydrogen concentrations up to 100%. This ability is attributed to the suppression of the α- to β-phase transition due to confinement effects in the extremely thin Pd layer. Since the maximal hydrogen-induced resistance change for the α-phase is 6%,[49] the sensitivity of this new type of sensor may be limited, resulting in stricter requirements on the signal-to-noise processing in the electrical circuits of the sensor device.

METHODS

Fabrication of Pd/Cr Nanowire Networks. Commercially available Anodisc13 membranes (Whatman Company)[41] with a nominal filtration pore diameter of 20 nm were cleaned in acetone for 10 min in an ultrasonic bath and then rinsed with deionized water followed with an ethanol rinse. They were dried using high-purity nitrogen gas.[37] Cr and Pd were sputtered sequentially onto the filtration membrane surface by employing an ACT-2400 thin film deposition system under a base vacuum of $\sim 1 \times 10^{-7}$ Torr. The working gas was argon (Ar) at a pressure of 3 mTorr. The deposition rates of Cr and Pd were 0.49 and 1.3 Å/s, respectively, determined by an *in situ* quartz crystal microbalance (QCM) thickness monitor (model TM-350 from Maxtek, Inc.). The sputtering time for a deposited metal was defined by using a desired nominal thickness divided by the deposition rate. A reference film was prepared for each nanowire network sample by placing a silicon substrate (with an oxide top layer of 300 nm) nearby during sputtering.

Scanning Electron Microscopy (SEM). A high-resolution field emission scanning electron microscope (FESEM) (Hitachi S-4700II) was used to image the morphology of the fabricated samples. The samples were mounted on an aluminum holder with double-sided carbon tape. The sample's top surface coated with Pd/Cr was also connected to the sample holder with double-sided carbon tape to avoid charging effects.

Hydrogen Sensing. Rectangle-shaped samples with width of 2 ± 0.5 mm were cut from the Pd/Cr-coated filtration membrane and glued onto a sample holder with the Pd/Cr nanowire networks facing up. Four electrical contacts were made to the sample with silver paste, and the distances between the two voltage leads are 3 ± 1 mm.[37] The H_2 sensor testing was performed by placing the sample in a sealed flow cell with a total dead volume of 2−3 mL. An array of ultrafast solenoid valves (response time of 25 ms) and minimized dead volume of the gas passages were used to accurately characterize these sensors with response times down to tens of milliseconds. H_2 gas (Airgas, ultrahigh purity or with concentrations of 0.1, 1, or 10% balanced with N_2) was premixed with N_2 gas (Airgas, ultrahigh purity) to the desired concentrations using mass flow controllers (Aalborg GFC17A). The purging gas is N_2. The total gas flow rate was 200 sccm. The resistance of the sample was measured in constant current mode with a current source (Keithly 6221), which can provide current from tens of nanoamperes to a few milliamperes. The voltage was recorded with a precision high-speed digital-to-analog (DAC) board (NI6259, 16 bits, sampling rate up to 1 MS/s) *via* a voltage preamplifier (Stanford Research Systems, SR560). All tests were carried out at room temperature.

Acknowledgment. The work on nanowire network fabrication was supported by the Department of Energy (DOE) Grant No. DE-FG02-06ER46334. J.P., H.H.W., U.W., G.W.C., and W.K.K. were supported by DOE BES under Contract No. DE-AC02-06CH11357. X.Q.Z. acknowledges partial support by the Nanoscience Fellowship of Northern Illinois University. We are grateful to Michael P. Zach and Phillip Stone for their technical assistance. The thin film deposition and morphological analyses were performed at the Center for Nanoscale Materials (CNM) and Electron Microscopy Center (EMC) of Argonne National Laboratory which is funded by DOE BES under Contract No. DE-AC02-06CH11357.

REFERENCES AND NOTES

1. Ramanathan, M.; Skudlarek, G.; Wang, H. H.; Darling, S. B. Crossover Behavior in the Hydrogen Sensing Mechanism for Palladium Ultrathin Films. *Nanotechnology* **2010**, *21*, 125501.
2. http://www1.eere.energy.gov/hydrogenandfuelcells/mypp/index.html.
3. Tabib-Azar, M.; Sutapun; Petrick, B. R.; Kazemi, A. Highly Sensitive Hydrogen Sensors Using Palladium Coated Fiber Optics with Exposed Cores and Evanscent Filed Interaction. *Sens. Actuators, B* **1999**, *56*, 158–163.
4. Crabtree, G. W.; Dresselhaus, M. S.; Buchanan, M. V. The Hydrogen Economy. *Phys. Today* **2004**, *57*, 39–44.
5. Jardine, A. P. Hydrogen Sensors for Hydrogen Fuel Cell Applications; http://www.powerpulse.net/techPaper.php?paperID=99.
6. Buttner, W. J.; Post, M. B.; Burgess, R.; Rivkin, C. An Overview of Hydrogen Safety Sensors and Requirements. *Int. J. Hydro. Energy* **2011**, *36*, 2462–2470.
7. Kong, J.; Chapline, M. G.; Dai, H. J. Functionalized Carbon Nanotubes for Molecular Hydrogen Sensors. *Adv. Mater.* **2001**, *13*, 1384–1386.
8. Favier, F.; Walter, E. C.; Zach, M. P.; Benter, T.; M. Penner, R. M. Hydrogen Sensors and Switches from Electrodeposited Palladium Mesowire Arrays. *Science* **2001**, *293*, 2227–2231.
9. Walter, E. C.; Favier, F.; Penner, R. M. Palladium Mesowire Arrays for Fast Hydrogen Sensors and Hydrogen-Actuated Switches. *Anal. Chem.* **2002**, *74*, 1546–1553.
10. Tibuzzi, A.; Di Natale, C.; D'Amico, A.; Margesin, B.; Brida, S.; Zen, M.; Soncini, G. Polysilicon Mesoscopic Wires Coated by Pd as High Sensitivity H_2 Sensors. *Sens. Actuators, B* **2002**, *83*, 175–180.
11. Varghese, O. K.; Gong, D.; Paulose, M.; Ong, K. G.; Dickey, E. C.; Grimes, C. A. Extreme Changes in the Electrical Resistance of Titania Nanotubes with Hydrogen Exposure. *Adv. Mater.* **2003**, *15*, 624–627.
12. Varghese, O. K.; Gong, D.; Paulose, M.; Ong, K. G.; Grimes, C. A. Hydrogen Sensing Using Titania Nanotubes. *Sens. Actuators, B* **2003**, *93*, 338–344.
13. Xu, T.; Zach, M. P.; Xiao, Z. L.; Rosenmann, D.; Welp, U.; Kwok, W. K.; Grabtree, G. W. Self-Assembled Monolayer Promoted Hydrogen Sensing of Ultra-thin Palladium Films. *Appl. Phys. Lett.* **2005**, *86*, 203104.
14. Paulose, M.; Varghese, O. K.; Mor, G. K.; Grimes, C. A.; Ong, K. G. Unprecedented Ultra-high Hydrogen Gas Sensitivity in Undoped Titania Nanotubes. *Nanotechnology* **2006**, *17*, 398–402.
15. Ding, D. Y.; Chen, Z. Volume-Expansion-Enhanced Pinning of Nanoporous Pd Films for Detection of High-Concentration Hydrogen. *Sens. Lett.* **2006**, *4*, 331–333.
16. Ding, D. Y.; Chen, Z. A Pyrolytic, Carbon-Stabilized, Nanoporous Pd Film for Wide-Range H_2 Sensing. *Adv. Mater.* **2007**, *19*, 1996–1999.
17. Khanuja, M.; Varandani, D.; Mehta, B. R. Pulse Like Hydrogen Sensing Response in Pd Nanoparticle Layers. *Appl. Phys. Lett.* **2007**, *91*, 253121.
18. van Lith, J.; Lassesson, A.; Brown, S. A.; Schulze, M.; Partridge, J. G.; Ayesh, A. A Hydrogen Sensor Based on Tunneling between Palladium Clusters. *Appl. Phys. Lett.* **2007**, *91*, 181910.
19. Sun, Y.; Wang, H. H. High-Performance, Flexible Hydrogen Sensors That Use Carbon Nanotubes Decorated with Palladium Nanoparticles. *Adv. Mater.* **2007**, *19*, 2818–2820.

20. Kiefer, T.; Favier, F.; Vazquez-Mena, O.; Villanueva, G.; Brugger, J. A. Single Nanotrench in a Palladium Microwire for Hydrogen Detection. *Nanotechnology* **2008**, *19*, 125502.
21. Joshi, R. K.; Krishnan, S.; Yoshimura, M.; Kumar, A. Pd Nanoparticles and Thin Films for Room Temperature Hydrogen Sensor. *Nanoscale Res. Lett.* **2009**, *4*, 1191–1196.
22. Yang, F.; Taggart, D. K.; Penner, R. M. Fast, Sensitive Hydrogen Gas Detection Using Single Palladium Nanowires That Resist Fracture. *Nano Lett.* **2009**, *9*, 2177–2182.
23. Jeon, K. J.; Jeun, M.; Lee, E.; Lee, J. M.; Lee, K. I.; von Allmen, P.; Lee, W. Finite Size Effect on Hydrogen Gas Sensing Performance in Single Pd Nanowires. *Nanotechnology* **2009**, *19*, 495501.
24. Offermans, P.; Tong, H. D.; van Rijn, C. J. M.; Merken, P.; Brongersma, S. H.; Crego-Calama, M. Ultralow-Power Hydrogen Sensing with Single Palladium Nanowires. *Appl. Phys. Lett.* **2009**, *94*, 223110.
25. Khanuja, M.; Kala, S.; Mehta, B. R.; Kruis, F. E. Concentration-Specific Hydrogen Sensing Behavior in Monosized Pd Nanoparticle Layers. *Nanotechnology* **2009**, *20*, 015502.
26. Yang, F.; Taggart, D. K.; Penner, R. M. Joule Heating a Palladium Nanowire Sensor for Accelerated Response and Recovery to Hydrogen Gas. *Small* **2010**, *6*, 1422–1429.
27. Yang, F.; Kung, S. C.; Cheng, M.; Hemminger, J. C.; Penner, R. M. Smaller Is Faster and More Sensitive: The Effect of Wire Size on the Detection of Hydrogen by Single Palladium Nanowires. *ACS Nano* **2010**, *4*, 5233–5244.
28. Agar, P.; Mehta, B. R.; Varandani, D.; Prasad, A. K.; Kamruddin, M.; Tyagi, A. K. Sensing Response of Palladium Nanoparticles and Thin Films to Deuterium and Hydrogen: Effect of Gas Atom Diffusivity. *Sens. Actuators, B* **2010**, *150*, 686–691.
29. Kiefer, T.; Villanueva, L. G.; Fargier, F.; Favier, F.; Brugger, J. The Transition in Hydrogen Sensing Behavior in Non continuous Palladium Films. *Appl. Phys. Lett.* **2010**, *97*, 121911.
30. Kiefer, T.; Villanueva, L. G.; Fargier, F.; Favier, F.; Brugger, J. Fast and Robust Hydrogen Sensors Based on Discontinuous Palladium Films on Polyimide, Fabricated on a Wafer Scale. *Nanotechnology* **2010**, *21*, 505501.
31. Zou, J.; Iyer, K. S.; Raston, C. L. Hydrogen-Induced Reversible Insulator−Metal Transition in a Palladium Nanosphere Sensor. *Small* **2010**, *6*, 2358–2361.
32. Lu, C.; Chen, Z MOS Hydrogen Sensor with Very Fast Response Based on Ultra-thin Thermal SiO_2 Film. *Int. J. Hydro. Energy* **2010**, *35*, 12561–12567.
33. Garzon, F. H. Development and Testing of a Miniaturized Hydrogen Safety Sensor. *Sens. Actuators, B* **2010**, *148*, 469–477.
34. Lee, J. M.; Lee, W. Effects of Surface Roughness on Hydrogen Gas Sensing Properties of Single Pd Nanowires. *J. Nanosci. Nanotechnol.* **2011**, *11*, 2151–2154.
35. Kim, K. R.; Noh, J.-S.; Lee, J. M.; Kim, Y. J.; Lee, W. Suppression of Phase Transitions in Pd Thin Films by Insertion of a Ti Buffer Layer. *J. Mater. Sci.* **2011**, *46*, 1597–1601.
36. Noh, J. S.; Lee, J. M.; Lee, W. Low-Dimensional Palladium Nanostructures for Fast and Reliable Hydrogen Gas Detection. *Sensors* **2011**, *11*, 825–851.
37. Zeng, X. Q.; Latimer, M. L.; Xiao, Z. L.; Panuganti, S.; Welp, U.; Kwok, W. K.; Xu, T. Hydrogen Gas Sensing with Networks of Ultrasmall Palladium Nanowires Formed on Filtration Membranes. *Nano Lett.* **2011**, *11*, 262–268.
38. Knight, B.; Clark, T. Development of Sensors for Automotive PEM-Based Fuel Cells; http://www.lanl.gov/orgs/mpa/mpa11/FinalReportforDOESensorsContractUTRC.pdf.
39. Liu, R.-J.; Crozier, P. A.; Smith, C. M.; Hucul, D. A.; Blackson, J.; Salaita, G. *In Situ* Electron Microscopy Studies of the Sintering of Palladium Nanoparticles on Alumina During Catalyst Regeneration Processes. *Microsc. Microanal.* **2004**, *10*, 77–85.
40. Baker, R. T. K.; Prestridge, E. B.; McVicker, G. B. The Interaction of Palladium with Alumina and Titanium-Oxide Supports. *J. Catal.* **1984**, *89*, 422–432.
41. Xiao, Z. L.; Han, C. Y.; Welp, U.; Wang, H. H.; Kwok, W. K.; Willing, G. A.; Hiller, J. M.; Cook, R. E.; Miller, D. J.; Crabtree, G. W. Fabrication of Alumina Nanotubes and Nanowires by Etching Porous Alumina Membranes. *Nano Lett.* **2002**, *2*, 1293–1297 and references therein.
42. Crispin, R. M.; Nicholas, M. The Wetting and Bonding Behaviour of Some Nickel Alloy-Alumina Systems. *J. Mater. Sci.* **1976**, *11*, 17–21.
43. Asthana, R.; Mileiko, S. T.; Sobczak, N. Wettability and Interface Considerations in Advanced Heat-Resistant Ni-Based Composites. *Bull. Pol. Acad. Sci.: Tech. Sci.* **2006**, *54*, 147–166.
44. Welp, U.; Xiao, Z. L.; Jiang, J. S.; Vlasko-Vlasov, V. K.; Bader, S.; Crabtree, G. W.; Liang, J.; Chik, H.; Xu, J. Superconducting Transition and Vortex Pinning in Nb Films Patterned with Nanoscale Hole-Arrays. *Phys. Rev. B* **2002**, *66*, 212507.
45. Xiao, Z. L.; Han, C. Y.; Welp, U.; Wang, H. H.; Vlasko-Vlasov, V. K.; Kwok, W. K.; Willing, G. A.; Miller, D. J.; Hiller, J. M.; Cook, R. E.; Crabtree, G. W. Nickel Antidot Arrays on Alumina Substrates. *Appl. Phys. Lett.* **2002**, *81*, 2869–2871.
46. Kulkarni, A. K.; Chang, L. C. Electrical and Structural Characteristics of Chromium Thin Films Deposited on Glass and Alumina Substrates. *Thin Solid Films* **1997**, *301*, 17–22.
47. Matula, R. A. Electrical Resistivity of Copper, Gold, Palladium, and Silver. *J. Phys. Chem. Ref. Data* **1979**, *8*, 1147.
48. Ealet, B.; Robrieux, B; Gillet, E. A. Surface Analytical Study of the Formation and Adhesion of Chromium Films on Alumina. *J. Adhes. Sci. Technol.* **1992**, *6*, 1221–1231.
49. Sakamoto, Y.; Takai, K.; Takashima, I.; Imada, M. Electrical Resistance Measurements as a Function of Composition of Palladium−Hydrogen (Deuterium) Systems by a Gas Phase Method. *J. Phys.: Condens. Matter* **1996**, *8*, 3399–3411.
50. Thomas, R. C.; Hughes, R. C. Sensors for Detecting Molecular Hydrogen Based on Pd Metal Alloys. *J. Electrochem. Soc.* **1997**, *144*, 3245–3249.
51. Suleiman, M.; Jisrawi, N. M.; Dankert, O.; Reetz, M. T.; Bahtz, C.; Kirchheim, R.; Pundt, A. Phase Transition and Lattice Expansion during Hydrogen Loading of Nanometer Sized Palladium Clusters. *J. Alloys Compd.* **2003**, *356−357*, 644–648.
52. Sachs, C.; Pundt, A.; Kirchheim, R.; Winter, M.; Reetz, M. T.; Fritsch, D. Solubility of Hydrogen in Single-Sized Palladium Clusters. *Phys. Rev. B* **2001**, *64*, 075408.
53. Di Vece, M.; Grandjean, D.; Van Bael, M. J.; Romero, C. P.; Wang, X.; Decoster, S.; Vantomme, A.; P. Lievens, P. Hydrogen-Induced Ostwald Ripening at Room Temperature in a Pd Nanocluster Film. *Phys. Rev. Lett.* **2008**, *100*, 236105.